The Selective OH Radical Oxidation of Sorbitylfurfural: A Combined Experimental and Theoretical Study

Salvatore S. Emmi,*,† Mila D'Angelantonio,† Gabriella Poggi,‡ Marialuisa Russo,† Giancarlo Beggiato,† and Bo Larsen§

Istituto di Fotochimica e Radiazioni d'Alta Energia (FRAE) del CNR, Area della Ricerca, Via P. Gobetti 101, I-40129 Bologna, Italy, Dipartimento di Chimica "G. Ciamician", Università di Bologna, Via G. Selmi 2, I-40126 Bologna, Italy, and Environment Institute, Joint Research Centre, TP290,21020 Ispra, Varese, Italy

Received: November 26, 2001; In Final Form: February 14, 2002

Sorbitylfurfural (Furalglucitol), widely used in the cosmetic industry as antioxidant and antiinflammatory agent, reacts with hydroxyl radical in neutral aqueous solution with a rate constant almost at the diffusional limit, $k_1 = 7.3 \times 10^9$ M^{-1} s^{-1}. Despite the unselective character of the OH radical, addition to the 5′ position in the furanic ring seems to provide the dominant path. The consequent allylic radical undergoes the cleavage of the C−O bond ($k_2 = 1.7 \times 10^6$ s^{-1}) in β position to form a pseudo-seven-atom ring via a hydrogen bond between the attacking OH group and the furanic oxygen. A 1,6 H-shift between the two oxygen atoms ($k_3 = 1.4 \times 10^5$ s^{-1}) then precedes a disproportionation reaction which leads to the final products ($k_4 = 2.0 \times 10^7$ M^{-1} s^{-1}). The proposed mechanism is based on the UV−vis spectra of intermediates and final products obtained after pulse and gamma radiolysis, on nonlinear kinetic fittings of absorbance versus time curves, on quantum-mechanical calculations of electronic transitions and reaction enthalpies. The two most important final products have been isolated and characterized as sorbityl-but-2-enal derivatives by LC-MS.

Introduction

Sorbitylfurfural (designated SF), shown in Chart 1, is an antioxidant molecule currently used with success in the topical treatment of dermatitis, and as such is a component of a line of antiinflammatory and antiaging creams. Its antiinflammatory action, associated with an excellent tolerance, provides a welcome alternative to cortisone and nonsteroid drugs whenever the latter cause skin sensitization or gastric conditions.[1] Its tetrasubstituted homologue, the 2,4-tetra-*o*-methyl-furfuryliden-sorbitol, has been shown to prevent liver-damaging effects of CCl_4, ethionin, allyl alcohol, and amanita phalloides.[1] Also, its antiinflammatory mechanism represents an alternative path to the inhibition of prostaglandins, i.e., the hormones released whenever a tissue is injured. Several in vitro investigations have led to postulate that the antiinflammatory effectiveness of SF be due to its radical inhibition property, without preventing the natural synthesis of prostaglandins.[3] It can be hypothesized that its mechanism of action blocks the OH radicals produced by hydroperoxidase during the autoxidation of arachidonic acid, which is the starting compound for the natural synthesis of prostaglandins and thromboxanes. By means of luminescent experiments in vivo, it has also been shown that a combination of 3% SF hydrophilic and 3% vitamin E-acetate hydrophobic has a synergic photoprotection effect on skin tissue.[4]

Sorbitylfurfural is a cyclic acetal due to the condensation of two natural substances, D-sorbitol (contained in sorb), and

CHART 1

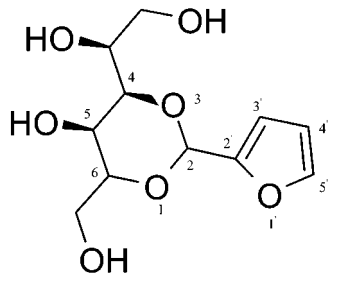

furfural (contained in bran), which, used separately or combined, have shown different biological activity.

A brief examination of the radical behavior of the two isolated components is a precondition toward the understanding of the novel chemical characteristics of the condensed molecule.

D-Sorbitol has been used for a long time in cosmetic creams and lotions, toothpastes and resins, as food additive, and for ascorbic acid fermentation. Its interaction with radicals has been studied in the context of polyhydric alcohols and sugars degradation, to the comprehension of which radiation chemical techniques gave a fundamental contribution. The radiation induced free radical reactions of carbohydrates have been comprehensively reviewed in the past and plausible mechanisms for their degradation have been proposed from the analysis of end products.[5,6] Also, transient studies have been done by conductivity,[7] and optical measurements.[8,9] Spin trapping has been employed with success by Kuwabara et al.[10] to identify the radicals formed in the reaction of five carbohydrates (glycerol-d_8, xylitol, dulcitol, D-sorbitol, and D-mannitol). The general conclusion reached is that carbohydrates show a very weak reactivity toward the hydrated electron and a fast reactivity with the OH radical. The latter is supposed to abstract hydrogen

* Corresponding author. Istituto FRAE-CNR, Area della Ricerca, Via P. Gobetti 101, 40129 Bologna, Italy. Tel.: + 39 0516399774. Fax: + 39 0516399848. E-mail: emmi@frae.bo.cnr.it.

† Istituto di Fotochimica e Radiazioni d'Alta Energia (FRAE) del CNR.

‡ Dipartimento di Chimica "G. Ciamician".

§ Environment Institute.

10.1021/jp014304z CCC: $22.00
Published on Web 04/17/2002

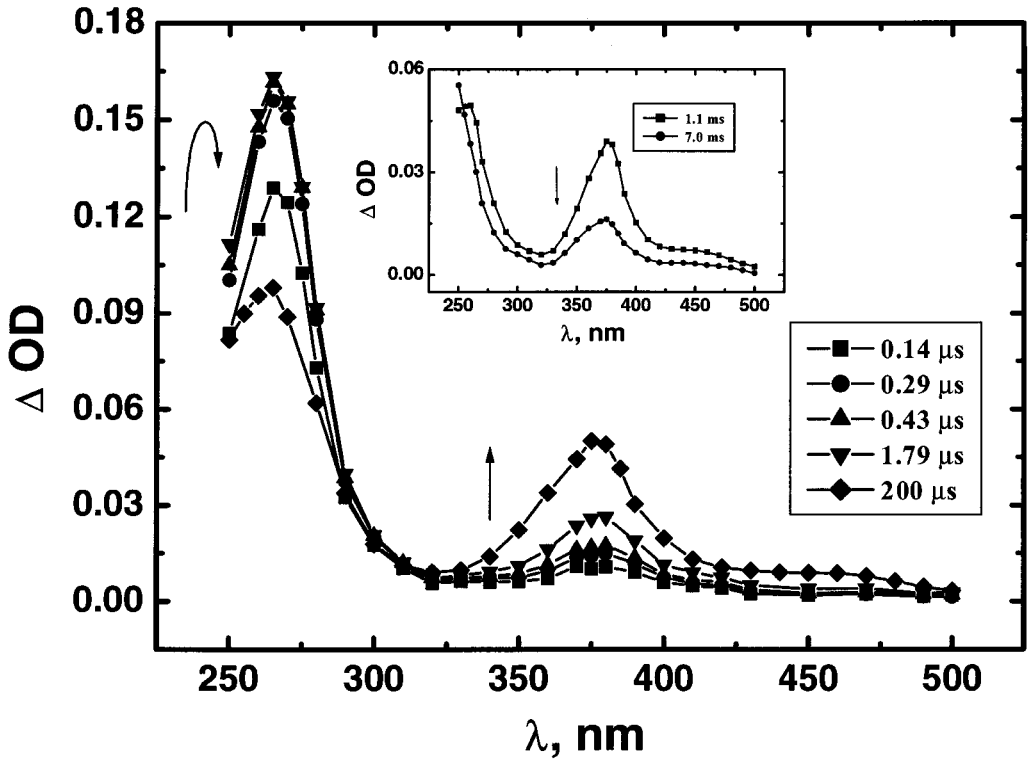

Figure 1. Time-resolved spectra of intermediates obtained after pulse radiolysis of a solution of [sorbitylfurfural] = 2 mM, N_2O saturated solution, natural pH. Curved arrow indicates a bleaching after an absorbance growth. Dose = 11 Gy, pulse length = 20 ns, optical path = 5 cm. Inset: long time region.

atoms mainly from C−H groups rather than from O−H groups. As it was expected from the "high reactivity−lack of selectivity" principle, most of these studies evidenced that a mixture of primary and secondary radical products are formed after OH attack, with a certain prevalence of the more stable glucosidic radicals centered in position C2. Kuwabara et al.,[10] definitely demonstrated the preferential formation of a primary carbon hydroxyalkyl radical (C1 position) in the five carbohydrates above (hence in D-sorbitol too), arguing that the C2 acylalkyl radical CHO−˙CH−CHOH follows from water elimination, rather than from direct H abstraction. Oxy- and deoxy-compounds, constituted by smaller fragments are found among the final products, but larger molecules are found as well in deoxygenated solutions.

Furfural is extracted from agricultural wastes and is widely used in the industry of plastics, rubber, petroleum, and vegetable oil. It is considered to be a potential biocompatible alternative to petrochemicals, but recently, it was also claimed[11] to participate to a cyclic reaction which leads to the production of hydrogen peroxide, known to be responsible for acid pollution. Thus its chemical impact on the environment is still under investigation. In the past furfural, together with furan, was the subject of a limited number of attempts to gather information on the nature and mechanistic behavior of the radical intermediates. Two of them concluded that OH addition is followed by the opening of the furanic ring.[12,13] Other two papers reported few kinetic data from competitive methods on the same process.[14,15] In a previous paper[16] we tried to clarify the course of OH attack to furfural, both by spectroscopic-kinetic pulse radiolysis and by calculating the energetics of the various steps. A preferential addition to C5 on the furanic ring, and the opening of the ring were found consistent with an overall mechanistic model, in which a fundamental role is played by a hydrogen shift between the two tails of the open ring itself. The rate constant of ring breakage resulted somewhat lower than that for furan,[13] i.e., $k_3 = (4.7 \pm 2.4) \times 10^5\ s^{-1}$ at neutral pH.

When we first tackled the study of the mechanism of the radical behavior of SF, we realized that the acetalic linkage between the furanic ring and the carbohydrate moiety modified the reaction channels of D-sorbitol with OH. The presence of the furanic ring seemed to guide the radicals in a preferential position on the ring itself, inhibiting the importance of any concurrent reaction path on the sugar carbons. Therefore we report herein a comprehensive study of the attack of OH radical to SF, started by means of both pulsed and stationary radiolytic methods in oxygen free aqueous solutions at their natural pH (5.5−6.0). This pH is chosen to give a mechanistic description of the SF antioxidant activity at the same physiological pH of the cosmetic line above. The subsequent rearrangements of the radical products were followed with spectrophotometric methods and the final products were identified by means of LC-MS. The kinetic path was then modeled and fitted to the experimental absorbance−time curves. Moreover, quantum mechanical calculations have been performed to define the geometry and the spectral properties of intermediates and final products, to check the consistency of the identity of products with their production energies, and to account for the experimental spectra by their simulation on the basis of excitation energies, oscillator strengths, and computed concentrations.

Results and Discussion

1. OH Attack. SF in concentrations ranging from 1×10^{-4} to 5×10^{-3} M was investigated by pulse radiolysis of N_2O saturated aqueous solution at natural pH, thus converting aqueous electrons into OH (G(OH) = 5.8). In these conditions, a small amount (10%) of H radical is produced (G(H) = 0.55) besides OH, but as its reactions are usually close to those of OH,[17] they will not be specifically considered in this paper. The

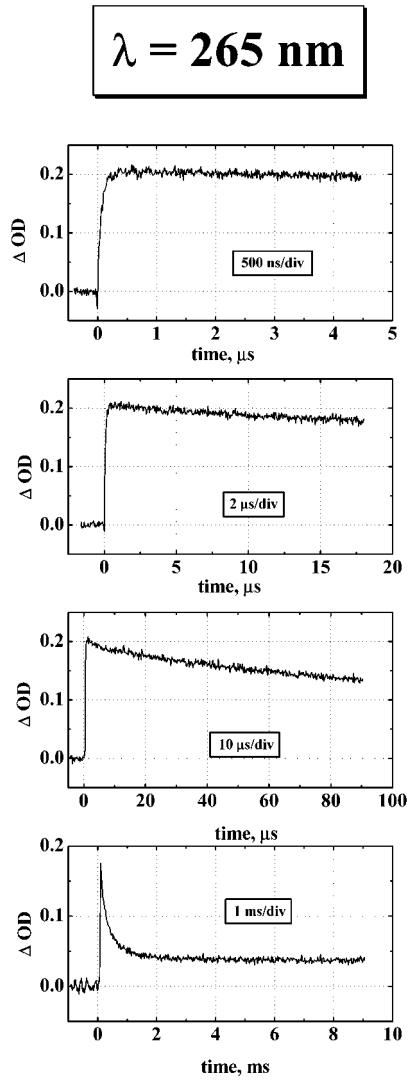

Figure 2. Sequence of the processes observed at 265 nm at different time scales, natural pH. Dose = 14 Gy, optical path = 5 cm, and [sorbitylfurfural] = 2 mM.

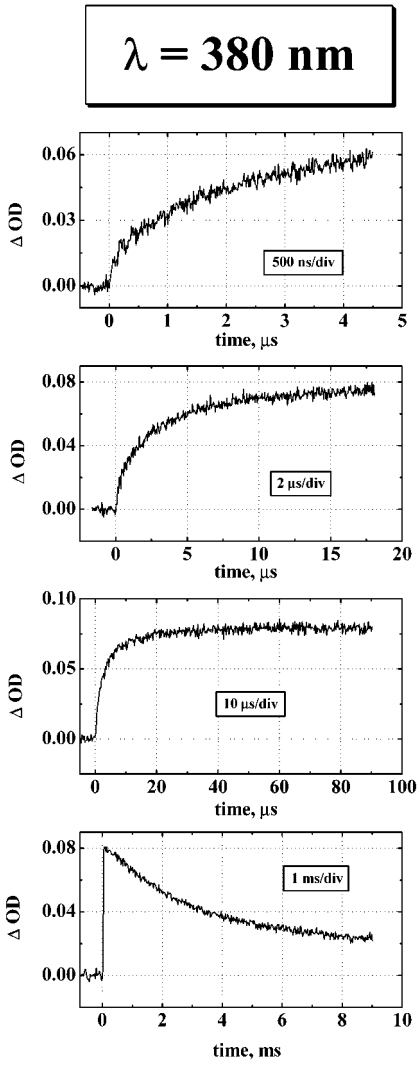

Figure 3. Sequence of the processes observed at 380 nm at different time scales, natural pH. Dose = 14 Gy, optical path = 5 cm, and [sorbitylfurfural] = 2 mM.

capture of OH is 100% complete when the SF concentration is ≥2 mM.

Observations of changes induced by pulse irradiation in the UV−vis spectra of the system have been expanded on a time window of 6 orders of magnitude (Figure 1), i.e., from a hundredth of nanoseconds to 200 μs (main spectra) down to the millisecond region (inset). The spectra of transients produced are characterized by two prominent absorptions at 265 and 380 nm which do not evolve equally in time: while the higher energy band grows up to 500 ns and then begins a slow decay, the latter (380 nm band) continues to increase for hundreds of microseconds before decaying.

The reaction with OH is diffusion controlled and depends linearly on the concentration of sorbitylfurfural, corresponding to a bimolecular rate constant of $k_1 = 7.3 \times 10^9$ M^{-1} s^{-1}.

Due to the well-known unselective character of OH radicals, a range of reactions is plausible, from hydrogen abstraction to ring attack or electron transfer. Furthermore, regarding hydrogen abstraction and ring attack, a statistic distribution of the attack site on the sorbitol hydrogens and the ring carbons is generally expected. It is then required that the kinetic analysis considers a wide variety of processes and products.

$$\text{OH} + \text{sorbitylfurfural} \rightarrow \text{products} \qquad (1)$$

The sequence of optical traces at the two characteristic λ's 265 and 380 nm is helpful in clarifying the time behavior of the mentioned bands (Figures 2 and 3). The first trace of Figure 2 shows that a very fast OH attack on the system takes place during the first 500 ns when the sample contains 2 mM SF. After that, the species absorbing at 265 nm undergo a long decay lasting milliseconds and leave a residual weak absorption. At 380 nm, on the other hand (Figure 3), the absorption keeps growing after the pulse for ca. 40 μs. Then the signal persists for 200 μs and only later decays, precisely on a time scale of tens of milliseconds, i.e., the process is 10 times as long as that observed at 265 nm. The residual absorption is also shown in the inset of Figure 1.

The reaction of sorbitol with OH was investigated as well and compared with the SF results. The OH attack on sorbitol produced an unstructured band from 220 to ca. 400 nm, probably the tail of a band peaking in the far UV. The build-up kinetics at 220 nm was followed as a function of sorbitol concentration and a reaction rate constant $k_{(\text{OH+sorbitol})} \sim 2 \times 10^9$ M^{-1} s^{-1} was derived.[18]

There is no similarity between the absorption bands of the OH-adducts related to sorbitol and sorbitylfurfural. The latter instead shows bands similar to those of the OH adduct to furfural,[16] both with regard to shape and time behavior. With

SCHEME 1: Sorbitylfurfural Oxidation Sequence Initiated by OH Radical

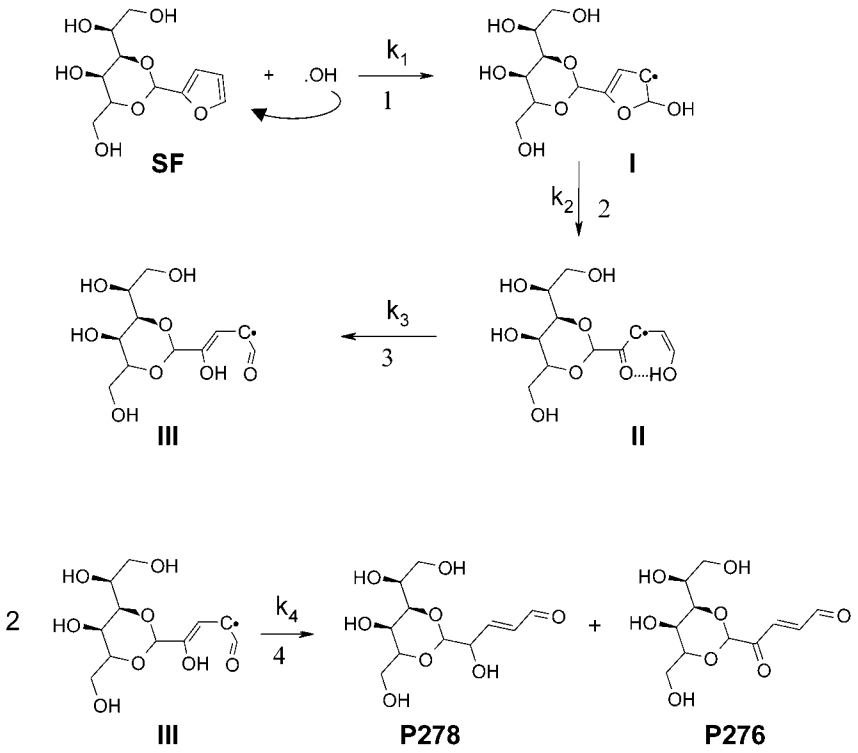

this compound, the two most significant bands were found at lower energies than with sorbitylfurfural, i.e., at 315 and 400 nm, but they stay approximately in the same intensity relationship as in the present case, and evolve in time in the same way, i.e., the UV band increases and then decreases, while the less energetic band continues to grow. The time frame is also corresponding.

2. Processes Involving the OH Adduct. In the case of furfural,[16] the analysis of the energetics of different OH reaction routes, which might lead either to an adduct, an acylic radical, or a radical cation, allowed us to conclude that addition in position 5 was the favorite path. A similar scheme was therefore applied to the present study, in which the OH radical is supposed to attack the furanic group in position 5′ producing an allylic radical on carbon 4′ (**I**). The allylic radical undergoes a C−O bond β-cleavage and quickly rearranges to a pseudo-7-atom ring (**II**) assisted by the establishment a H-bond between two oxygen atoms: the first from the hydroxyl group (*outer oxygen*) and the latter from an incoming carbonyl group (*inner oxygen*). The establishment of a hydrogen-bond is predicted by a H···O distance shorter than 3.2 Å and an angle O−H···O wider than 150° (the optimized values are 1.72 Å and 155.1°, respectively). A thorough discussion regarding the transformations occurring in the furanic ring is reported in the previous paper.[16] The chance of an α-cleavage is very remote because it requires the formation of a carbene intermediate, which was computed to be a rather high endothermic process.[16] A third step consists of H-transfer from the outer to the inner oxygen and formation of a new carbonyl bond at the outer oxygen (**II**). The fourth step is the termination reaction, which, as it will be discussed in the following section, turns out to be a disproportionation of **III**. The reaction scheme is illustrated in Scheme 1.

3. Curve Fitting. The kinetic model has been submitted to a curve-fitting procedure at both wavelengths 265 and 380 nm for different SF concentrations and doses. Some known parameters were fixed, as the OH recombination rate, and the extinction coefficients of sorbitylfurfural, ($\epsilon_{265} = 0$, $\epsilon_{380} = 0$), whereas all the other kinetic and spectral parameters were optimized to obtain the best fit (Figure 4). The OH attack is best illustrated by Figure 4a at 265 nm, however the sole analysis at this λ would not have permitted to distinguish OH attack from ring opening since, as it turns out, radicals **I** and **II** have very close extinction coefficient values (4200 and 4300 M^{-1} cm^{-1} at 265 nm, respectively) (Table 1). Instead, these processes can be better monitored at 380 nm (Figure 4b) where the extinction coefficient values of the two intermediates vary almost by a factor of 3 (see Table 1 and spectra from 0.29 to 1.79 μs in Figure 1). The fitting of the final decay is shown in Figure 4c and Table 1 reports the results. The goodness of fitting is high for each step, being indicated by a very low reduced-χ^2 value, i.e., $10^{-4}-10^{-6}$, and by the symmetrical distribution of residuals around zero (see insets in Figure 4). It is worth to note that SF reacts with OH somewhat faster ($k = 7.3 \times 10^9$ M^{-1} s^{-1}) than sorbitol and furfural (respectively, $k = 2.2 \times 10^9$ and 4.7×10^9 M^{-1} s^{-1}). Also the reorganization of the radical adduct seems to have been accelerated by the presence of the sorbitol chain. Particularly the influence on its stability is evidenced by the fact that ring breaks three times faster ($k_2 = 1.7 \times 10^6$ s^{-1}) than in the furfural instance ($k = 4.7 \times 10^5$ s^{-1}) and the following transfer of hydrogen is four times faster ($k_3 = 1.4 \times 10^5$ s^{-1} with respect to a furfural $k = 3.4 \times 10^4$ s^{-1}). As the production enthalpies of **II** are very similar for the two compounds, the difference may be thought to arise from a larger entropic contribution in the carbonyls formation in the case of sorbitylfurfural.[19]

The termination reaction is instead 15 times slower for SF and may reflect a greater difficulty in achieving the right orientation for disproportionation.

4. Identification of End Products. Gamma radiolysis was employed at natural pH, to produce the end products deriving from the reactions of OH with SF and its separate components sorbitol and furfural. The irradiation was limited to the range where consumption of reagents is linear with dose, and generally it did not exceed the 20% of their initial concentration. This

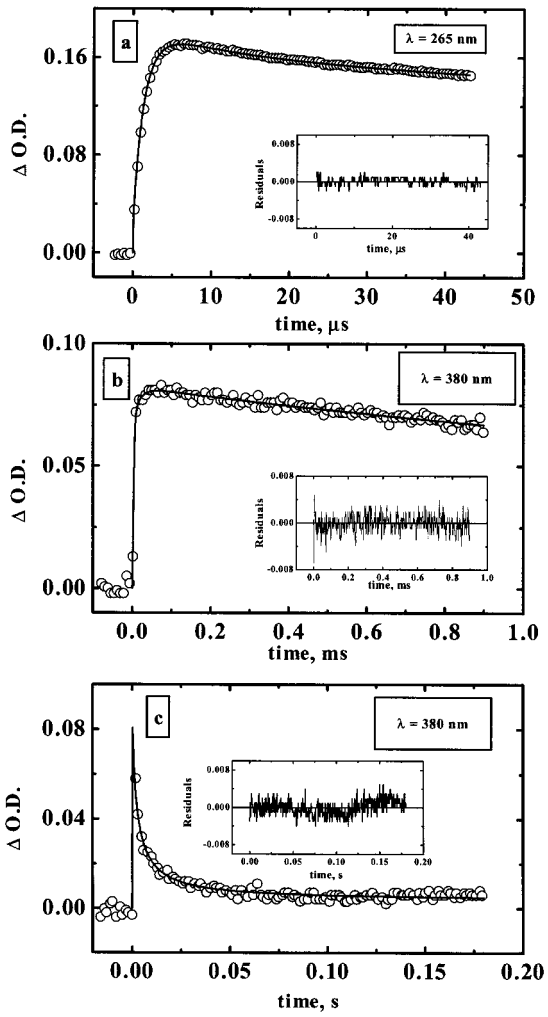

Figure 4. Output of the best fitting of the reaction model reported in Scheme 1: (a) [sorbitylfurfural] = 1×10^{-4} M, $\lambda = 265$ nm, dose = 17 Gy, optical path = 5 cm, goodness of fitting $\chi^2 = 4.2 \times 10^{-6}$; (b) [sorbitylfurfural] = 2×10^{-3} M, $\lambda = 380$ nm, dose = 14 Gy, optical path = 5 cm, goodness of fitting $\chi^2 = 4.14 \times 10^{-5}$; (c) [sorbitylfurfural] = 2×10^{-3} M, $\lambda = 380$ nm, dose = 14 Gy, optical path = 5 cm, goodness of fitting $\chi^2 = 4.65 \times 10^{-4}$.

TABLE 1: Optimized Kinetic Constants and Extinction Coefficients[a]

kinetic constants	ϵ at 265 nm (M^{-1} cm^{-1})	ϵ at 380 nm (M^{-1} cm^{-1})
$k_1 = (7.3 \pm 0.9) \times 10^9$ M^{-1} s^{-1}	**I**: (4200 ± 600)	**I**: (330 ± 25)
$k_2 = (1.7 \pm 0.02) \times 10^6$ s^{-1}	**II**: (4300 ± 640)	**II**: (950 ± 360)
$k_3 = (1.4 \pm 0.9) \times 10^5$ s^{-1}	**III**: (3000 ± 930)	**III**: (1500 ± 390)
$k_4 = (2.0 \pm 0.2) \times 10^7$ M^{-1} s^{-1}	final products: (1000 ± 150)	final products: (120 ± 40)

[a] By facsimile; assumptions: 100% OH capture, and sorbitylfurfural extinction coefficients, ϵ_{265} and $\epsilon_{380} = 0$; error limits represent two standard deviations.

precaution ensures that the products we are examining are related to the reactions of the title compound and not to byproducts accumulated during irradiation.

Spectrophotometric Methods. Figure 5 shows the spectral measurements after progressive irradiations. Figure 5a is related to a low concentration (100 μM) of SF and shows that its consumption at 212 nm, matches the appearance of a new band centered at 250−260. With more concentrated samples (2 mM), irradiation can be extended to higher doses such that the band reveals to be well structured and peaking at 254 nm (Figure 5b). This band is stable after irradiation and then characterizes the end products; moreover the inlet of molecular oxygen into the sample does not alter the absorption, proving that products are no longer radical in nature.

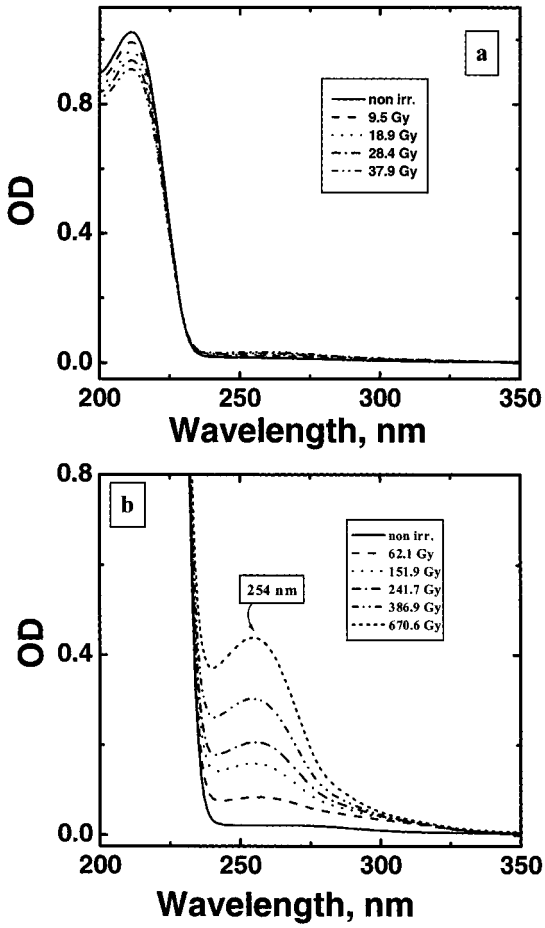

Figure 5. UV−vis spectra after progressive gamma irradiation of sorbitylfurfural, N_2O saturated solutions, natural pH: (a) 0.1 mM, (b) 2 mM. Doses as inside the figure.

As the two products formed from the fourth step of Scheme 1 are stable carbonyl compounds, they accumulate during continuous radiolysis and can produce the spectrum shown in Figure 5b. A support to this hypothesis comes from the consistency of the extinction coefficients of the products obtained with the two different irradiation methods: after pulse radiolysis the best fitting (see Table 1) calculates an $\epsilon_{265} \sim 1000$ $M^{-1}cm^{-1}$, about the same value found after γ-radiolysis from the data of Figure 5b.

By means of the methylindole method, it was ascertained that free malonaldehyde is not one of the products. Deoxy-compounds were also searched by means of the periodic acid oxidation method (see Experimental Section). This very sensitive method proved that only traces of deoxy-compounds are present (a *G*-value as low as 0.06 was found) in agreement with Scherz data related to a series of different carbohydrates.[20] Absence of furfural was also ascertained spectrophotometrically: in fact furfural shows an unequivocal characteristic band centered at 278 nm, which was not detected at all in the samples under study. If on one hand these results seem to indicate that the sugar skeleton is not particularly involved in the OH attack, on the other hand they need further support to conclude that OH reaction mainly follows the path of Scheme 1. Therefore a more comprehensive investigation was carried out by means of LC-MS^n on the stable products after irradiation.

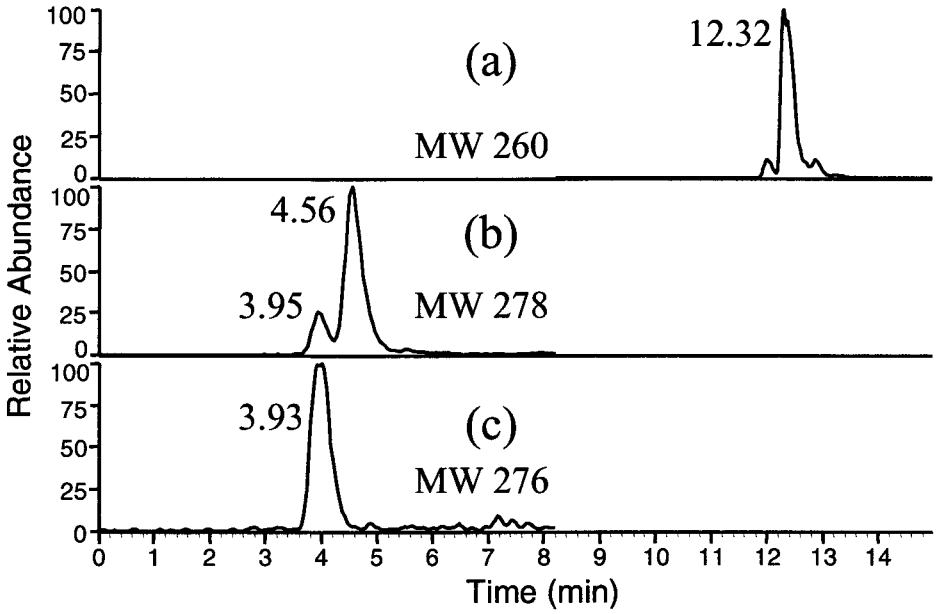

Figure 6. Liquid Chromatograms of a γ-irradiated solution of [sorbitylfurfural] = 20 mM, dose = 6.6 kGy, dilution 1:20.

LC-MS^n. The samples for LC-MS^n analysis were obtained by irradiating a N_2O saturated aqueous solution containing 20 mM SF with γ-rays with a dose of 6.6 kGy, which resulted in a consumption of SF in the order of 20%. Samples taken before and after irradiation were diluted 100 and 20 times, respectively, with 50% water in methanol.

Four peaks are observed in the chromatogram of irradiated SF (Figure 6) one of which derives from residual SF (MW = 260). Two other major peaks and a minor peak elute 8−9 min before SF and are characterized by higher molecular weights (MW = 276 and 278), which is in good accordance with oxidation products of SF containing an extra oxygen and water molecule (ΔM = 16 and 18). This finding may be explained by a disproportionation reaction as the one proposed in Scheme 1 (reaction 4), which would produce two major peaks, one at MW 278 (a hydroxylic product) and the second at MW 276 (the carbonylic counterpart). The additional minor peak with MW = 278 may derive from a structural isomer of the hydroxylic product.

The MS^n analysis of SF, and the two isomers seen as small shoulders on the chromatographic peak, revealed the sequence (*m*/*z* 259 → *m*/*z* 163 → *m*/*z* 131 → *m*/*z* 101) (Figure 7a), which corresponds to a fragmentation pathway in which molecular furfural is first eliminated followed by methanol and formaldehyde (see Supporting Information, Scheme 1S).

The MS^n analysis of the major reaction product with the molecular weight 278 produced a major fragment ion at *m*/*z* 113, and minor fragment ions at *m*/*z* 163, 131, and 101 (Figure 7b and Supporting Information, Scheme 2S). Additional small fragment ions were seen at *m*/*z* 229 (loss of H_2O and HCHO) and at *m*/*z* 161, which may derive from loss of molecular hydrogen from the fragment at *m*/*z* 163. The MS^n spectra of the minor product with the molecular weight 278 contained a number of ions in addition to those of the major isomeric product. These ions may not be genuine fragments from the minor product but may derive from other compounds with MW = 278 present in the background.

The analysis of the reaction product with the molecular weight 276 gave the sequence (*m*/*z* 275 → *m*/*z* 161; *m*/*z* 113) (Figure 7c and Supporting Information, Scheme 3S). The main difference in the spectrum of this product with respect to that of the 278-product is caused by the presence of a very acidic hydrogen in the central part of the structure, which increases the possibilities of creating a carbanion and may lead to a different fragmentation pathway.

5. Energetics of reactions and Calculation of the UV−Visible Spectra. Since the evolution of UV−vis spectra with time closely follows that observed for furfural,[16] the kinetic model fits the experimental traces and the LC-MS analyses are consistent with the final products proposed in Scheme 1, the energetics of reactions 1−4 has been examined thoroughly. The optimization of the various molecules investigated has been carried out at the HF/3-21G* level, and the respective energies have been improved with MP2/3-21G*//HF/3-21G* and HF/6-31G*//HF/3-21G* evaluations. The nature of true minima was in all cases confirmed through HF/3-21G* frequency computations, which allowed also to estimate the required thermodynamic quantities such as enthalpies. The exothermicity of each of the various reaction steps was considered as an indication of its likelihood. While all methods gave negative reaction enthalpies for the OH attack and for the H-transfer (the third reaction), only the most sophisticated theoretical approach of the three gave a negative reaction enthalpy for step 2 (ring opening) and step 4 (disproportionation), showing the importance of correlation in distinguishing between nearly degenerate systems.

These results, presented in Table 2, are considered consistent with the proposed mechanism.

Spectra. Once a reasonable interpretation of the energetics has been established, the second step consists of predicting the contribution to the overall spectra of the various species involved in the process. Of course, the first system investigated is sorbitylfurfural itself. The ZINDO/S computed spectrum (Figure 8) shows a single line at 213 nm, the experiment yielding a single peak at 212 nm (Table 3). Table 3 also contains the calculated electronic transitions and oscillator strengths for the postulated intermediates and final products, which are seen to fall within the experimental region, i.e., bands centered at 265, 380, and ~450 nm.

As the mechanism consists of a series of consecutive reactions, forming and decaying intermediates contribute to the shape and intensity of experimental bands by summing their individual contributions. Thus a true comparison of theoretical

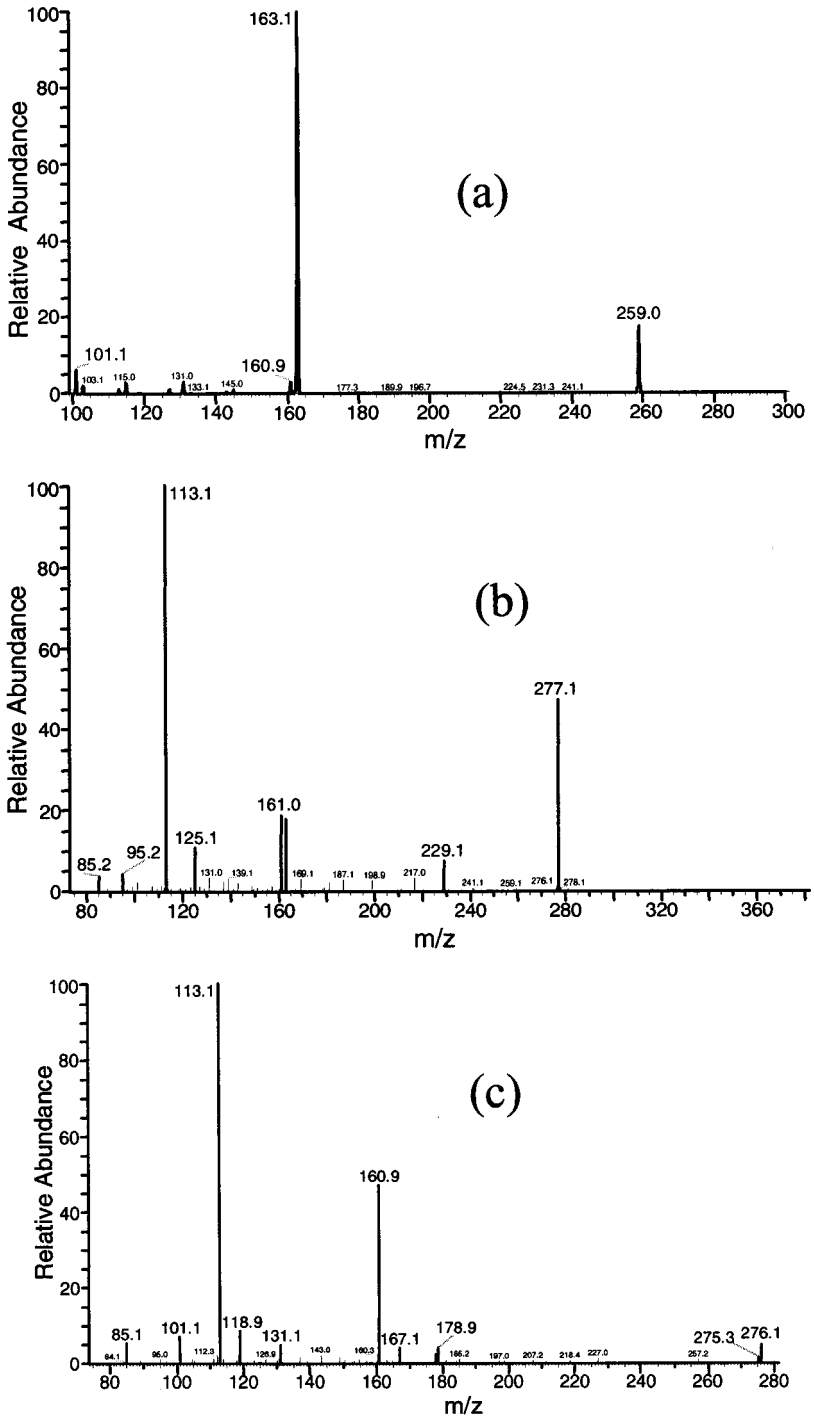

Figure 7. APCI(−)-MS^2 spectra of (a) unirradiated sorbitylfurfural, (b) the peak at retention time 4.56 min, MW = 278, and (c) the peak at retention time 3.93 min, MW = 276.

with experimental bands requires a reconstruction of the pulse radiolysis spectra at the considered time of the process. To this purpose the concentrations of each species, as determined by the curve-fitting method, was taken into account. The reconstruction has been carried out at the two key times of 0.14 and 1.79 μs elapsed after the pulse. The former (0.14 μs) represents that stage of the process when the hydroxylated radical **I** is mostly responsible for the 265 and 380 nm peaks: i.e., the addition reaction is still in course while a small amount of adduct molecules have been affected by the β-cleavage of the carbon−oxygen bond in the furanic ring. The computed optical spectrum, normalized to the absorption maximum of the 265 nm experimental peak, is shown in Figure 9a.

At the latter key time of 1.79 μs, when the absorption reaches its maximum in the UV and the 380-peak is still growing, three species are believed to be simultaneously present, namely **I**, **II**, and **III**. That is, in terms of active processes: all OH is almost consumed to form an allylic radical on the furanic ring, the ring opening is already occurring, and the H-shift from *outer*- to *inner*-oxygen has began. After the convolution of the spectral contributions pertaining to the three species, their sum appears in Figure 9b. The experimental spectrum is reproduced satisfactorily, both with respect to the position of the bands and to their evolution with time. In particular, the ratio of band intensities A_{265}:A_{380} decreases with time as observed experimentally. The two shoulders, appearing in the reconstructed

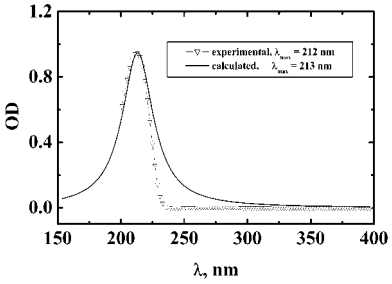

Figure 8. UV−vis spectrum of sorbitylfurfural experimental and calculated. [sorbitylfurfural] = 1.00×10^{-4} M, optical path = 1 cm.

TABLE 2: Reaction Enthalpies

reaction	method	ΔH (kcal/mol)
SF + OH $\xrightarrow{k_1}$ **I**	HF/3-21G*//HF/3-21G*	−44.05
	MP2/3-21G*//HF/3-21G*	−40.19
	HF/6-31G*//HF/3-21G*	−30.62
I $\xrightarrow{k_2}$ **II**	HF/3-21G*//HF/3-21G*	+0.18
	MP2/3-21G*//HF/3-21G*	+0.11
	HF/6-31G*//HF/3-21G*	−0.72
II $\xrightarrow{k_3}$ **III**	HF/3-21G*//HF/3-21G*	−17.04
	MP2/3-21G*//HF/3-21G*	−17.50
	HF/6-31G*//HF/3-21G*	−1.52
2 **III** $\xrightarrow{k_4}$ P276 + P278	HF/3-21G*//HF/3-21G*	+64.39
	MP2/3-21G*//HF/3-21G*	+5.82
	HF/6-31G*//HF/3-21G*	−3.23

TABLE 3: Spectral Data Concerning the Products of Reactions 1−4[a]

species	calcd electronic transitions (nm)	oscillator strength	exptl bands (nm)
sorbityl-furfural	213	0.32	212
I	254, 388, 430	0.034, 0.037, 0.001	265, 380, ∼450
II	262, 273, 294, 419	0.1, 0.034, 0.08, 0.08	265, 380, ∼450
III	285, 422	0.19, 0.065	265, 380, ∼450
P276	246	0.59	254
P278	229	0.57	254

[a] Hyperchem-ZINDO/S: convergence limit = 0.0001; overlap weighting factors: $\sigma-\sigma = 1.267$; $\pi-\pi = 0.505$; CI occupied and unoccupied orbitals = 12 × 12.

spectrum at the right of the main peaks, are due to transitions computed at 285−294 and 419−422 nm, which may result from a ZINDO/S overestimation of the oscillator strengths in the former case, or to a red-shift effect of solvation on the radical species (the 450 nm band visible in Figure 1), in the case of the lower energy band.

Conclusions

The identified final products from OH reactions with deoxygenated solutions of SF have to be accounted for by disproportionation reactions of radicals formed after a series of rearrangements. These include the cleavage of the C−O bond of the furanic ring in the β-position and the 1,6 H-shift from two oxygen atoms. Neither direct electron transfer, nor hydrogen abstraction seem to take a noticeable part in the process (if these reactions occur at all), but an attack on position 5′ of the furanic ring dominates all plausible processes generally considered in the radiolysis of carbohydrates.[6] It has to be supposed that a lower energy reaction channel is activated when the sugar skeleton is connected to the furanic ring with a cyclic acetalic linkage. With respect to furfural alone, the presence of the carbohydrate chain accelerates the reorganization of the hydroxylated radicals, and slows down the termination reaction. No dimers or higher weight molecular species have been found, as might be eventually expected in deoxygenated solutions, if the radicals were located on the carbohydrate chain. Instead, the process terminates with a disproportionation reaction, the products of which are identified as two sorbitylbutenal derivatives, namely a 4-hydroxy-but-2-enal product (the reduced one) and a 4-oxo-but-2-enal product (the oxidized one).

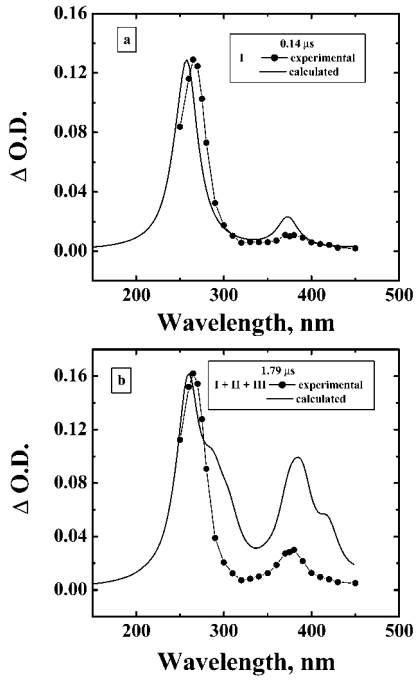

Figure 9. Comparison of experimental and computed spectra of pulse irradiated sorbitylfurfural at two key times of the degradation process (a) 0.14 μs and (b) 1.79 μs. Computed absorptions were normalized to the experimental maximum. Each computed absorbance contribution accounts for the concentration of the species calculated with the parameters listed in Table 1. The experimental spectra are the same reported in Figure 1 at the appropriate times.

A sum of different approaches have been applied, varying from laboratory's tests, like LC-MS analysis, to theoretical calculations, and all of them give support to a four-steps radical degradation process of sorbitylfurfural.

The investigation also proposes the carbohydrate moiety, condensed with a furanic derivative, as a structure liable to undergo a selective oxidation induced by the OH radical. At the present, work is in progress to establish which role oxygen plays, when the system is exposed to radical attack in aerated conditions.

Experimental Section

1. Materials. Sorbitylfurfural (99.7%), $C_{11}H_{16}O_7$, CAS no. 7089-59-0, also known as furalglucitol and AR-GB11 appears, under the form of white crystalline flakes soluble in water and was used as received from Laboratori Fitocosmesi & Farmaceutici, Milan. Its UV−vis spectrum is reported in Figure 8 and shows an absorption peak at 212 nm where the extinction coefficient measures $\epsilon_{212} = 9473\ M^{-1}cm^{-1}$. D-Sorbitol (Fluka MicroSelect) was used as received as well. Solutions were prepared with Millipore (Milli-Q) water, purged with Argon, and then saturated with N_2O. The natural pH of the system was 5.5−6.0. SF is stable in aqueous solution between pH's 5 and 9. At more acidic pH's it undertakes hydrolysis to the free components sorbitol and furfural. As usual for the acetals, SF is attacked by bases only at very high pH's.

2. Radiolysis. Pulse radiolysis experiments were performed by using the 12 MeV linear accelerator (Linac) at the FRAE Institute.[21] Details on the optical detection system, methods and computer treatment of data are described elsewhere.[22] Ten to 50 ns pulses delivering doses from 3 to 70 Gy were used. The radiation dose per pulse was monitored by means of a charge collector plate calibrated with an O_2 saturated solution of 0.1 M KSCN and by taking $G\epsilon_{500\ nm} = 2.15 \times 10^4$ (100 eV)$^{-1}$ $M^{-1}cm^{-1}$, where G and ϵ are respectively the radiation yield and extinction coefficient for the $(SCN)_2^{-\cdot}$ radical (the *G*-value is defined as the number of molecules transformed per 100 eV of radiation energy absorbed). The rate constant of e^-_{aq} with SF is very low, $k \ll 10^7\ M^{-1}\ s^{-1}$. Therefore at the concentrations used, SF cannot compete for e^-_{aq} with N_2O. Gamma radiolysis was performed with a ^{60}Co γ-cell and dosimetry was done with a standard Fricke dosimeter. The pH of a typical sample after gamma irradiation was 5.9, practically at the physiological value as desired. Absorption spectra of samples were recorded with a Perkin-Elmer Lambda 9 spectrophotometer and Perkin-Elmer Lambda 40.

3. Quantum Mechanical Methods. Geometry optimizations of radicals and stable products were performed by using the Gaussian98[23] on a Digital Alpha PW 433 au, at the HF level, utilizing a 3-21G* basis. The energies of the optimized structures were then refined by single point calculations at the 6-31G* level. Excited states were computed semiempirically with the ZINDO/S Hamiltonian,[24] yielding excitation energies and oscillator strengths. However, the direct utilization of the ab initio optimized geometries as input to ZINDO/S computations produced meaningless results, namely a number of "excited states" having negative energies. Apparently the presence of many low-frequency modes produced a significant difference in the ground-state geometries of the two theoretical schemes. Better, meaningful results were obtained by reoptimizing geometries at PM3 level. The number of MOs involved in the CI was 12 occupied and 12 virtual ones. Finally, the spectral data thus obtained were convoluted to output a qualitative representation of the UV−vis spectrum for each species considered: a Lorentzian expression was used to calculate, for each transition, the line-shape of the bands, which were then assembled to yield the spectrum.[25] The electronic transitions of SF itself were first computed in order to verify the reliability of the semiempirical method,[26] and were likewise convoluted so as to reproduce the spectrum. The agreement between experimental and computed bands gives some confidence with respect to the further application of the method to the species formed after irradiation.

4. Reaction Modeling Methods. Linear fitting was used to test whether simple kinetic models allow to interpret the behavior of optical densities vs time by using two programs developed in Asyst language.[27]

Nonlinear (curve) fitting was carried out by using the FACSIMILE chemical modeling package.[28] It uses numerical techniques and a special high-level programming language in which chemical reactions are expressed as ordinary differential equations. FACSIMILE contains a parameter-fitting option, whereby specified parameters can be adjusted with a recursive calculation to minimize the sum of the squares of all the residuals for all the data. For a numerical evaluation of the fitting quality the usual reduced-χ^2 parameter is reported in the legends of figures.

5. Product Analysis. End products have been analyzed spectrophotometrically in the UV−vis and by means of GC-MS (ion volume mass spectrometer Finnigan MAT GCQ) and LC-MS^n in the APCI (atmospheric pressure chemical ionization source) mode.[29,30] In the last case the aqueous samples (20 μL) were loop injected into a thermoseparation LC coupled to a Finnigan MAT LCQ ion-trap mass spectrometer. The LC was equipped with a 15 cm × 2.1 mm C_{18}-coated silica gel (5 μm). Discovery column (Supelco, Milan, Italy) run in the gradient mode (0.2 mL min^{-1}) at 20 °C. The eluent was a mixture of H_2O and methanol. The gradient program was: 0% methanol for 4 min followed by 0% to 50% methanol in 15 min. The outlet of the LC was interfaced to the ion trap through an atmospheric pressure chemical ionization source (APCI) run at 450 °C at a corona discharge voltage of +5kV. The sheath and auxiliary gases were N_2 and He, respectively. In a first run the ion trap was scanned from 70 to 400 *m*/*z* with three scans s^{-1}. In additional runs the ion trap was operated in the MS^n daughter ion scan mode (30% relative energy, wide band excitation) with the primary cycle(s) locked on the *m*/*z* value(s) corresponding to the *quasi*-molecular ion of the suspected target compounds or the fragment ion of interest and the daughter ions scanned from *m*/*z* 70 to ca. 10 amu above the molecular weight of the ion under investigation.

Two chemical methods were also employed to search for carbonylic groups. The first method was applied for the identification of malonaldehyde as a direct product of irradiation: the sample is treated with an acidified solution of 2-methylindole which transforms malonaldehyde into a red complex absorbing at 555 nm.[31] The second method was used to look for generic carbonyl compounds: these are oxidized to malonaldehyde treating the sample with periodic acid. Malonaldehyde is then complexed with 2-thiobarbituric acid to a complex absorbing at 532 nm.[32]

Acknowledgment. The skillful assistance of Dr. Eng. A. Martelli and Mr. A. Monti for the pulse radiolysis equipment and of Mr. L. Ventura for the technical workshop are greatly acknowledged. We also thank Laboratori Fitocosmesi & Farmaceutici srl (Milan) for financial support.

Supporting Information Available: Three detailed MS^n fragmentation schemes (Schemes 1S, 2S, and 3S) for sorbityl-furfural and for the final products. This material is available free of charge via the Internet at http://pubs.acs.org.

References and Notes

(1) Zanoli, P.; Baggio, G.; Poggioli, R. *Agents Actions* **1982**, *12*, 4−10.
(2) Garzia, A.; Zanoli, P. *Riv. Farmacol. Ter.* **1981**, *XII*, 153−154.
(3) Bader, S.; Carinelli, L.; Cavalletti, T.; Giuliani, A. L.; Traniello, S. *Int. J. Cosmet. Sci.* **1990**, *12*, 1−4.
(4) Gers-Barlag, H.; Mueller, A.; Uhlmann, B.; Sauermann, G.; Pfannenbecker, U.; Pape, W.; Wittern, K. P. Fural Glucitol and Vitamin E-acetate. A New Combination against Free Radicals in Human Skin. Poster presentation at the 18th International IFSCC Congress, Venice, Italy, October 3−6, 1994; P 037.
(5) Kochetkov, N. K.; Kubrjashov, L. I.; Chlenov, M. A. *Radiation Chemistry of Carbohydrates*; Pergamon: New York, 1979.
(6) von Sonntag, C. *Adv. Carbohydr. Chem. Biochem.* **1980**, *37*, 7−77.
(7) Bothe, E.; Schulte-Frohlinde, D.; von Sonntag, C. *J. Chem. Soc., Perkin Trans. 2* **1978**, 416−420.
(8) Moore, J. S.; Kemsley K. G.; Davies, J. V.; Phillips, G. O. In *Radiation Biology and Chemistry. Research Developments*; Edwards, H. E., Navaratnam, S., Parsons, B. J., Phillips, G. O., Eds.; Studies in Physical and Theoretical Chemistry 6; Elsevier: Amsterdam, 1979; pp 99−113.
(9) Goldstein, S.; Czapski, G. *Int. J. Radiat. Biol.* **1984**, *46*, 725−729.
(10) Kuwabara, M.; Zhang, Z.-Y.; Inanami, O.; Yoshii, G. *Radiat. Phys. Chem.* **1984**, *24*, 217−227.
(11) Anastasio, C.; Faust, B. C.; Rao, C. J. *Environ. Sci. Technol.* **1997**, *31*, 218−232.
(12) Schuler, R. H.; Laroff, G. P.; Fessenden, R. W. *J. Phys. Chem.* **1973**, *77*, 456−466.
(13) Lilie, J. *Z. Naturforsch.* **1971**, *26b*, 197−202.

(14) Savel'eva, O. S.; Shevchuk, L. G.; Vysotskaya, N. A. *J. Org. Chem. USSR* **1973**, *9*, 759−761.
(15) Vysotskaya, N. A.; Shevchuk, L. G.; Gavrilova, S. P.; Badovskaya, L. A.; Kul'nevich, V. G. *J. Org. Chem. USSR* **1983**, *19*, 1352−1354.
(16) D'Angelantonio, M.; Emmi, S. S.; Poggi, G.; Beggiato, G. *J. Phys. Chem.* **1999**, *103*, 858−864.
(17) Swallow, A. J. *Radiation Chemistry An Introduction;* Longman Group Limited: London, 1973; p 153.
(18) D'Angelantonio, M.; Emmi, S. S. Unpublished results.
(19) Wilt, J. W. *Free Radicals*; Kochi, J. K., Ed.; J. Wiley and Sons: New York, 1973; Vol. I, p 413.
(20) Scherz, H. *Radiat. Res.* **1970**, *43*, 12−24.
(21) Hutton, A.; Roffi, G.; Martelli, A. *Quad. Area Ric. Emilia-Romagna* **1974**, *5*, 67−74.
(22) Emmi, S. S.; D'Angelantonio, M.; Poggi, G.; Beggiato, G.; Camaioni, N.; Geri, A.; Martelli, A.; Pietropaolo, D.; Zotti, G. *Res. Chem. Intermed.* **1998**, *24*, 1−14.
(23) Frisch, M. J.; Trucks, G. W.; Schlegel, H. B.; Scuseria, G. E.; Robb, M. A.; Cheeseman, J. R.; Zakrzewski, V. G.; Montgomery, J. A., Jr.; Stratmann, R. E.; Burant, J. C.; Dapprich, S.; Millam, J. M.; Daniels, A. D.; Kudin, K. N.; Strain, M. C.; Farkas, O.; Tomasi, J.; Barone, V.; Cossi, M.; Cammi, R.; Mennucci, B.; Pomelli, C.; Adamo, C.; Clifford, S.; Ochterski, J.; Petersson, G. A.; Ayala, P. Y.; Cui, Q.; Morokuma, K.; Malick, D. K.; Rabuck, A. D.; Raghavachari, K.; Foresman, J. B.; Cioslowski, J.; Ortiz, J. V.; Baboul, A. G.; Stefanov, B. B.; Liu, G.; Liashenko, A.; Piskorz, P.; Komaromi, I.; Gomperts, R.; Martin, R. L.; Fox, D. J.; Keith, T.; Al-Laham, M. A.; Peng, C. Y.; Nanayakkara, A.; Gonzalez, C.; Challacombe, M.; Gill, P. M. W.; Johnson, B.; Chen, W.; Wong, M. W.; Andres, J. L.; Gonzalez, C.; Head-Gordon, M.; Replogle, E. S.; Pople, J. A. *Gaussian 98*, revision A.7, Gaussian, Inc.: Pittsburgh, PA, 1998.
(24) *HyperChem, Release 6 for Windows, Molecular Modeling Systems*; Hypercube, Inc.: Waterloo, Ontario, Canada, 2000.
(25) *Origin*, version 6.1*;* OriginLab Corp.: Northampton, MA, 2000.
(26) Del Bene, J.; Jaffe, H. H. *J. Chem. Phys.* **1968**, *48*, 4050−4055.
(27) (a) Camaioni, N.; Mulazzani, Q. Technical Report 8/93; Istituto FRAE-CNR: Bologna, Italy, 1993. (b) Camaioni, N.; Emmi, S. S.; Mulazzani, Q. Technical Report 9/93, version 1.0; Istituto FRAE-CNR: Bologna, Italy, 1993.
(28) *FACSIMILE for Windows*, version 3.0*;* AEA Technology plc: Harwell, Didcot, Oxfordshire, U.K., 1998.
(29) Zurek, G.; Luftmann H.; Karst, U. *Analyst* **1999**, *124*, 1291−1295.
(30) Kolliker, S.; Oehme, M.; Dye, C. *Anal. Chem.* **1998**, *70*, 1979.
(31) Scherz, H.; Stehlik, G.; Bancher, F.; Kaindl, K. *Mikrochim. Acta* **1967**, *5*, 915−919. Scherz, H.; Grunewald, Th. *Kerntechnik* **1970**, *11*, 501−503.
(32) Waravdekar, V. S.; Saslaw, L. D. *J. Biol. Chem.* **1959**, *234*, 1945−1950.